ORIGINAL PAPER

Titanium dioxide nanotube arrays modified with a nanocomposite of silver nanoparticles and reduced graphene oxide for electrochemical sensing

Wei Wang · Yibing Xie · Chi Xia · Hongxiu Du · Fang Tian

Abstract We report on a new nanocomposite material for electrochemical sensing of hydrogen peroxide using a titanium dioxide nanotube arrays modified with reduced graphene oxide onto which silver nanoparticles (AgNPs) were chemically deposited. Transmission electron microscopy, scanning electron microscopy, X-ray diffraction, and energy-dispersive X-ray and Raman spectroscopy were used to characterize its microstructure and morphology. The results demonstrated that the AgNPs were uniformly dispersed on the surface of the modified electrode which was investigated with respect to capability for sensing hydrogen peroxide (H_2O_2). Under optimized experimental condition, the electrode responds to H_2O_2 with a sensitivity of 1152 μA mM^{-1} cm^{-2} at a working potential of −0.6 V. The current response is linearly related to the concentration of H_2O_2 in the range from 50 to 15.5 mM (with a correlation coefficient of 0.9997), and the detection limit is 2.2 μM. The sensor exhibits good stability and excellent selectivity for H_2O_2. By immobilizing glucose oxidase on the surface of this electrode, a glucose biosensor was obtained that responds to glucose in the 0.5 to 50 mM concentration range.

W. Wang · Y. Xie · C. Xia · H. Du · F. Tian
School of Chemistry and Chemical Engineering, Southeast University, Nanjing 211189, China

W. Wang · Y. Xie (✉) · C. Xia · H. Du
Suzhou Research Institute of Southeast University, Suzhou 215123, China
e-mail: ybxie@seu.edu.cn

Introduction

Many types of nanomaterials, such as SiO_2, Al_2O_3, MnO_2 and TiO_2, have been used to construct biosensors [1–3]. Among them, the highly ordered TiO_2 nanotube arrays (TiO_2NTs) represent an excellent material with good biocompatibility, relatively high electrical conductivity, environmentally benign, inexpensive and large numbers of active reaction sites for chemical reactions [4, 5]. In particular, well aligned nanoarray structure can highly promote interfacial electron transportation and molecule/ion diffusion in an electrochemical process [6–9]. Therefore, TiO_2NTs can be regarded as an ideal substrate material to fabricate electrochemical biosensors [10, 11, 5]. However, the electrochemical sensors using pure TiO_2 nanomaterial often exhibit low sensitivity. Thus, the loading of catalytic materials such as various enzymes or noble metal nanoparticles on TiO_2 nanostructures becomes necessary. In addition, enzymeless TiO_2 based electrochemical sensors always show lower sensitivity than those prepared with enzymes [12]. Consequently, it is necessary and pressing to improve the sensitivity of such enzymeless electrochemical sensors.

Hybrid nanomaterials have been studied extensively because of their excellent physicochemical properties and the consequent broad spectrum of applications including targeted therapeutics, drug delivery and ultrasensitive detection. Some noble metal nanoparticles, particularly Au, Ag, and Pt, have attracted great attention because of their distinctive electrocatalytic property, excellent conductivity and larger specific surface area, and often are used for fabrication hybrid nanomaterials [13, 14]. Among them, Ag nanoparticles

(AgNPs) are widely and intensively investigated since the price of silver is much cheaper than the other mentioned noble metals and the conductivity is the best. Furthermore, the AgNPs are often used to modify TiO_2 materials for various applications such as glucose biosensors and hydrogen peroxide biosensors [10]. Up to now, lots of methods have been reported for the preparation of AgNPs-modified TiO_2NTs, such as microwave-assisted approach, photodeposition, electrodeposition and chemical reduction methods [10]. Unfortunately, AgNPs prepared by most of the existing techniques suffer from problems, including poor stability and reproducibility, due to unordered particles aggregation [15, 16]. As a result, the catalytic sites of AgNPs might be decreased. The high surface area to volume ratio of the nanoparticles results in high reactivity which leads to particle aggregation unless the nanoparticles are protected by capping agents that provide colloidal stability through electrostatic or steric repulsion. The balance between the van der Waals attraction forces and the electrostatic or steric repulsion forces determines the colloidal stability [17]. Accordingly, it is worthwhile to explore an effective agent-modified TiO_2NTs for preventing the AgNPs aggregation.

On the other hand, graphene, a new class carbon-based nanomaterial, comprising a two-dimensional single layer sheet of sp^2 bonded carbon atoms that are packed into a honeycomb structure, has attracted tremendous attention from both the experimental and the theoretical scientific communities [13, 18, 19]. This unique nanostructure exhibits excellent properties, such as fast electron transportation, chemical stability, mechanical strength, large surface-to-volume ratio, and good biocompatibility [20–22]. Graphene's favorable characteristics as mentioned above make it an attractive matrix for nanocomposites. To date, many articles about immobilization reduce graphene oxide (r-GO) or graphene oxide (GO) onto TiO_2NTs have been reported. For example, Liu et al. employed a cyclic voltammetric reduction process to reduce graphene oxide onto the TiO_2NTs [23]. Yun et al. presented a combined electrophoretic deposition-anodization approach to prepare a reduced graphene oxide-TiO_2NTs film [24]. Song et al. deposited the graphene oxide onto the surface of TiO_2NTs by a simple dip-and-dry method [25]. Additionally, it is reported that the aggregation of deposited nanoparticles on graphene sheets can be prevented by the strong van der Waals force between the graphene and nanoparticles, and the size of the obtained nanoparticles is usually small [26–28]. However, to our best knowledge, there are still few studies concerning modification of r-GO on the TiO_2NTs surface as a matrix for AgNPs deposition.

We report on a new nanocomposite material for electrochemical sensing application. The r-GO was used to modify TiO_2NTs to prevent the AgNPs aggregation, which ensured large specific surface area of the electrodes, and led to a higher sensitive electrochemical sensor. The AgNPs were chemi-deposited on r-GO-modified TiO_2NTs. The TiO_2NTs/r-GO/AgNPs

nanocomposite electrode was used for hydrogen peroxide detection. The electrochemical catalytic activity of the as-prepared electrode to H_2O_2 was evaluated systematically. Additionally, the nanocomposite electrode was also used for fabrication of glucose biosensor via immobilizing GOx onto its surface.

Experimental

Reagents and apparatus

Titanium sheet (Ti, purity> 99.95 %, thickness 0.25 mm) was purchased from Good fellow Cambridge Ltd (http://www.goodfellow.cn). Glucose oxidase (GOD, from Aspergillus Niger, 136,300 units/g solid, without added oxygen) was purchased from Sigma-Aldrich Co. (http://www.sigmaaldrich.com). Graphite powder, hydrogen peroxide (H_2O_2, 30 wt.%), D-(+) glucose, ammonia solution (25 wt.%), silver nitrate ($AgNO_3$), ascorbic acid, sucrose, L-histidine, dopamine, uric acid and other chemical reagents were purchased from Sinopharm Chemical Reagent Co., Ltd (http://www.sinoreagent.com) are analytical grade and used without further purification. Doubly distilled water was used throughout. All electrochemical experiments and measurements were carried out in N_2-saturated 0.2 M phosphate buffer solution at ambient temperature under stirring condition.

The phase of the TiO_2NTs/r-GO/AgNPs was determined by X-ray powder diffraction (XRD, Cu K_α=1.54056 Å, Rigaku/Dmax-2500, Japan, http://www.rigaku.com). The microstructure of r-GO was characterized by transmission electron microscopy (TEM, JEM-200CX, JEOL, Japan, http://www.jeol.co.jp). The morphologies of the nanomaterials were characterized by scan electron microscopy (SEM, Hitachi S-3000, Japan, http://www.hitachi.com). The energy-dispersive X-ray spectroscopy (EDS) spectrums were measured during the SEM measurements. Raman spectra were recorded on an in Via Raman microprobe (Renishaw Instruments, England, http://www.renishaw.com) with 514 nm laser excitation. Electrochemical experiments were performed with an electrochemical workstation (CHI 760D, Shanghai Chenhua, China, http://www.chinstruments.com). A three-electrode system was used in this process, which employed the bare and enzyme immobilized electrodes as the working electrodes, a platinum sheet as the counter electrode, and a saturated calomel electrode (SCE) as the reference. All potentials were referred to the SCE electrode.

Preparation of TiO_2NTs/r-GO/AgNPs nanocomposite electrode

TiO_2NTs were directly synthesized on titanium (Ti) sheet substrate by a potentiostatic anodization at 60 V for 3 h in

water and ethylene glycol mixture solution (volume ratio, 1:99) containing 0.25 wt% ammonium fluoride. A calcination treatment at 450 °C for 2 h was used for crystallization of TiO_2NTs from amorphous to anatase phase.

Graphene oxide (GO) was synthesized using a modified Hummer's method [29]. To form a GO solution, GO were dispersed in distilled water with the concentration of 5 mg mL^{-1}. The GO solution was sonicated in bath sonication for 60 min to form a stable GO suspension. The TiO_2NTs were immersed for 3 h in the stable GO suspension, since the GO can be absorbed on TiO_2NTs surfaces by physical absorption. Subsequently, the TiO_2NTs/GO was immersed in distilled water to remove unabsorbed GO, and then dried at room temperature. Afterward, TiO_2NTs/GO was immersed in hydrazine hydrate and water mixture solution (volume ratio, 1:1) and heated at 95 °C for 12 h. After that, the obtained TiO_2NTs/r-GO matrix was washed with distilled water several times then dried at room temperature.

The AgNPs were deposited on TiO_2NTs/r-GO matrix by a chemi-deposition process according to the previously reported method [30]. For obtaining $[Ag(NH_3)_2]^+$ solution, ammonia solution (2 wt.%) was dropwise added to $AgNO_3$ solution until it became transparent. Subsequently, the concentration of silver cation was adjusted to 0.1 M. After that, the TiO_2NTs/r-GO matrix was immersed in $[Ag(NH_3)_2]^+$ solution for 1 min. Then the substrate was immersed into distilled water for 10 s and then immersed in a glucose solution for 1 min. Afterward, the substrate was washed with distilled water to remove any glucose molecule. The preparation process of the TiO_2NTs/r-GO/AgNPs nanocomposite was schematically shown in Fig. 1. For a comparison, TiO_2NTs/AgNPs was also fabricated by the same preparation procedure of TiO_2NTs/r-GO/AgNPs nanocomposite as described above.
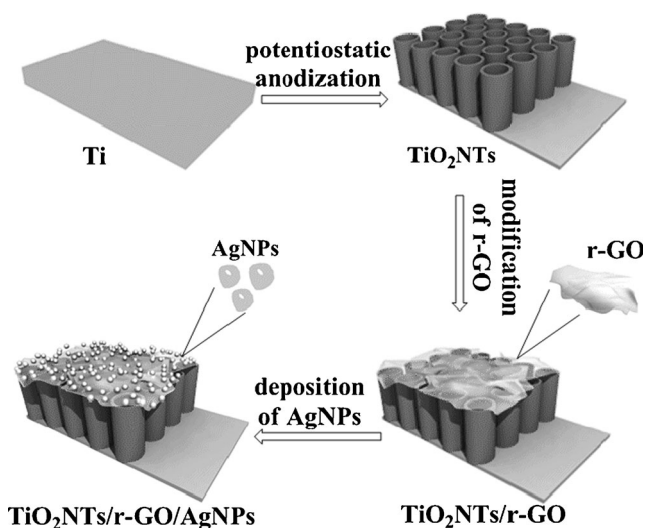

Fig. 1 Schematic showing the preparation of TiO_2NTs/r-GO/AgNPs nanocomposite

Results and discussion

Characteristics of materials

XRD pattern of the TiO_2NTs/r-GO/AgNPs nanocomposite is shown in Fig. S1 in the Electronic Supplementary Material (ESM). The peaks could be well indexed to those of anatase TiO_2 (JCPDS card No. 21–1272) and face-centered cubic Ag (JCPDS card No. 04–0783), indicating that the TiO_2 and Ag were all in the crystalline state.

The morphology of the r-GO was observed by TEM with JEM-200CX operating at 200 kV. Fig. 2 showed the TEM image of the r-GO nanosheet, illustrating clearly that the transparent sheets were flake-like with wrinkles. From the TEM image, it can be seen that r-GO was exfoliated into single or very thin layers.

Raman spectroscopy is a powerful, nondestructive tool, which is often used to differentiate the ordered and disordered crystalline structure of carbon materials, provided additional evidence of r-GO. The Raman spectroscopy of TiO_2NTs/r-GO was shown in Fig. S2 (ESM). It exhibited a strong D-band around 1,350 cm^{-1}, arising from a breathing mode of κ-point photons of A_{1g} symmetry, and a relatively weak G-band around 1,590 cm^{-1}, arising from the first order scattering of the E_{2g} phonon of sp^2 C atoms [31, 32]. The significant increase of D/G intensity ratio represented the decrease of the size of the in-plane sp^2 domains and partially disordered crystal structure of r-GO nanosheets [33]. The above results proved the formation of TiO_2NTs/r-GO matrix.

The surface morphology of different materials was investigated by SEM. Fig. 3a displayed the surface morphology of TiO_2NTs. The TiO_2NTs showed a highly ordered structure with an inner pore diameter of ~80 nm and a tube thickness of ~30 nm. In contrast, SEM of TiO_2NTs/r-GO (Fig. 3b) showed that nearly full surface of TiO_2NTs was covered by the transparent r-GO nanosheets. As seen in Fig. 3c, AgNPs were immobilized on the TiO_2NTs surface through a chemi-deposition process. However, lots of aggregations of AgNPs were also observed. The inserted image in Fig. 3c was the higher magnification image of TiO_2NTs/AgNPs. It showed that the diameter size of one single silver nanoparticle had a
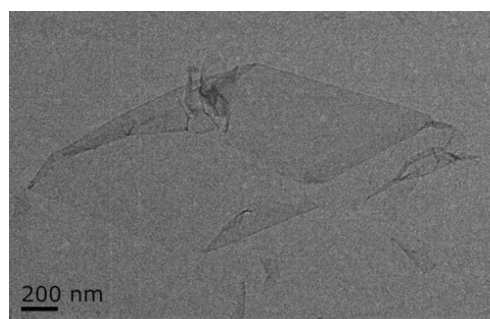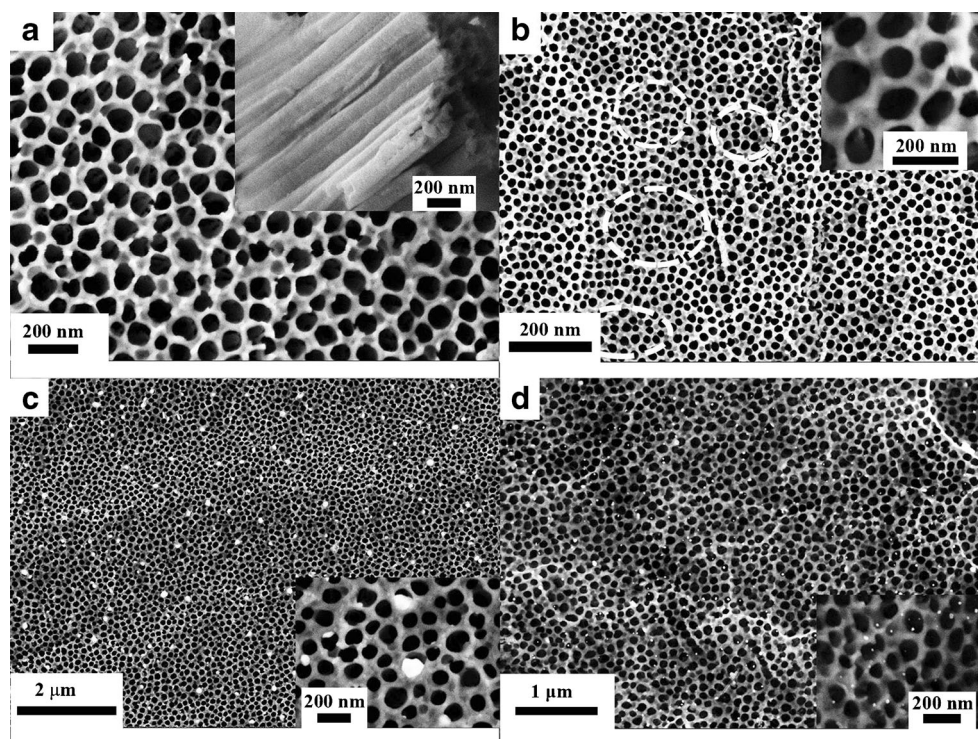

Fig. 2 TEM image of reduced graphene oxide

range of 30~100 nm. Fig. 3d showed the SEM image of TiO$_2$NTs/r-GO/AgNPs nanocomposite. The coverage of AgNPs on the surface of TiO$_2$NTs/r-GO matrix was denser than that on the surface of TiO$_2$NTs. The size of AgNPs was uniform and small, which had a range of 20~30 nm. That is to say, r-GO modified on TiO$_2$NTs was helpful for the uniform deposition of AgNPs and preventing AgNPs aggregation.

Fig. S3 (ESM) showed the EDS spectra of TiO$_2$NTs/AgNPs and TiO$_2$NTs/r-GO/AgNPs. EDS spectra exhibited signals of Ag with weight percentage of 2.58 % (Fig. S3A) and 3.47 % (Fig. S3B), respectively. The increased Ag weight percentage proved that the r-GO modification on TiO$_2$NTs could increase the effective surface for more AgNPs deposition.

Electrochemical performance of different electrodes

Cyclic voltammetric sensing of hydrogen peroxide

The electrocatalytic performance of the nanocomposite electrode towards the reduction of H$_2$O$_2$ in N$_2$-saturated phosphate buffer solution (pH 6.8) was investigated by cyclic voltammetric. The cyclic voltammograms of the nanocomposite electrode in N$_2$-saturated phosphate buffer solution from −0.8 to 0 V at a scan rate of 50 mV s^{-1} was shown in Fig. 4. A reduction peak at about −0.6 V (vs. SCE) was observed in the presence of 1 mM H$_2$O$_2$, which was corresponding to the electrochemical reduction of H$_2$O$_2$. Thus, the constant potential of −0.6 V was chosen as the optimum detection potential.

Amperometric response of the electrodes to H$_2$O$_2$

Based on the optimum conditions studied above, the application of the four kinds of electrodes in amperometric determination of H$_2$O$_2$ concentration had been investigated. The typical amperometric responses at the electrodes for each successive addition of 0.2 mM H$_2$O$_2$ were shown in Fig. S6 (ESM). The corresponding calibration curves were shown in Fig. 5. All sensors showed a sensitive response to the change of H$_2$O$_2$ concentration, indicating a good electrocatalytic property of four electrodes. The response current density of the TiO$_2$NTs/r-GO electrode (648.29 μA mM^{-1} cm^{-2}) was only a little higher than that of TiO$_2$NTs electrode (613.82 μA mM^{-1} cm^{-2}). However, the response current
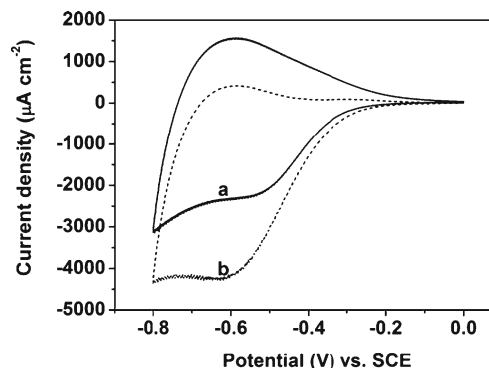

Fig. 4 Cyclic voltammograms (*CVs*) of the nanocomposite electrode **a** in the absence and **b** in the presence of 1 mM H$_2$O$_2$ in N$_2$-saturated 0.2 M phosphate buffer solution (pH 6.8) at the scan rate of 50 mV s^{-1}
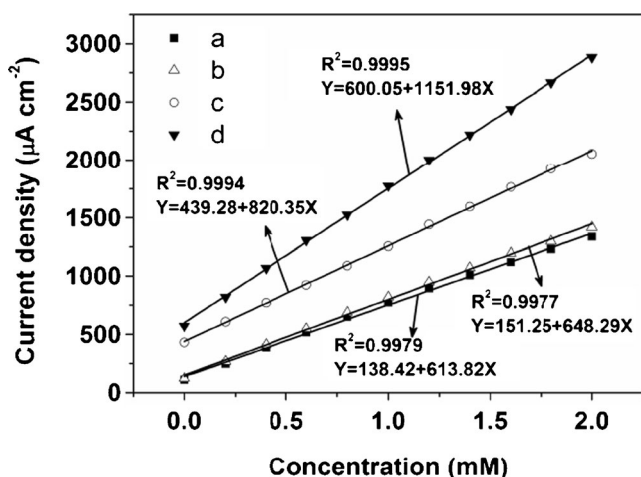
Fig. 5 Calibration curves for the amperometric response of **a** TiO$_2$NTs electrode, **b** TiO$_2$NTs/r-GO electrode, **c** TiO$_2$NTs/AgNPs electrode and **d** nanocomposite electrode during electro-reduction of H$_2$O$_2$

density of the TiO$_2$NTs/r-GO/AgNPs nanocomposite electrode reached 1151.98 μA mM^{-1} cm^{-2}, which was much higher than that of the TiO$_2$NTs/AgNPs (820.35 μA mM^{-1} cm^{-2}) electrode. So, the electrochemical activity of r-GO modified TiO$_2$NTs was almost similar to that of TiO$_2$NTs itself. However, the electrochemical activity of nanocomposite electrode was significantly higher than that of TiO$_2$NTs/AgNPs due to the increasing catalytic sites of small AgNPs. In other words, r-GO modification on TiO$_2$NTs surface was an effective way to the sensing performance of AgNPs deposited TiO$_2$NTs-based nanocomposite.

Similar experiments were conducted using the nanocomposite electrode with a successive addition of H$_2$O$_2$ to the N$_2$-saturated phosphate buffer solution at an applied potential of −0.6 V (vs. SCE) (Fig. S7A, ESM). Fig. S7B showed that nanocomposite electrode exhibited the linear response of H$_2$O$_2$ at a concentration range from 0.05 to 15.5 mM. A low detection limit of 2.2 μM was achieved at a signal to noise ratio of 3 (correlation coefficient R^2, 0.9997). As evidenced by the above experimental result, the nanocomposite electrode showed very good sensing performance.

A comparison of these analytical performances to the recent literature on TiO$_2$NTs-based H$_2$O$_2$ electrochemical sensors were shown in Table S1 in ESM. The sensitivity of the nanocomposite electrode was significantly higher than that of other TiO$_2$NTs-based H$_2$O$_2$ sensors. It means that the prepared nanocomposite electrode had a potential application in the determination of H$_2$O$_2$.

Interference, reproducibility, stability study and real sample analysis

An interference study is a very important aspect in the determination of any species by electrochemical methods. The selectivity of nanocomposite electrode was evaluated in the presence of common interfering electroactive substances such as ascorbic acid, sucrose, L-histidine, glucose, dopamine and uric acid in phosphate buffer solution. As shown in Fig. S8 (ESM), the current responses to 0.1 mM ascorbic acid, sucrose, L-histidine, glucose, dopamine and uric acid were negligible when compared to 0.5 mM H$_2$O$_2$. Thus, H$_2$O$_2$ sensor using this nanocomposite electrode exhibited highly selectivity for H$_2$O$_2$ detection.

In addition, the reproducibility and stability of the nanocomposite electrode were investigated in phosphate buffer solution. The relative standard deviation for three different electrodes was 4.68 % corresponding to 0.5 mM H$_2$O$_2$ under the same testing condition. These results proved that the fabrication procedure of the sensor was reliable and the H$_2$O$_2$ sensor was reproducible. Furthermore, after being stored for 60 days, the response to 0.5 mM H$_2$O$_2$ only decreased about 3.8 %, indicating the moderate stability of the constructed H$_2$O$_2$ sensor.

In order to assess the applicability during real sample analysis, the nanocomposite electrode was applied to determine H$_2$O$_2$ in human blood serum. The samples were diluted 1,000 times before determination. As shown in Table S2, the measured H$_2$O$_2$ concentrations were close to that of stoichiometrically added H$_2$O$_2$. The results suggested that the nanocomposite electrode could be used to determine H$_2$O$_2$ in serum.

Preparation of enzyme electrode

It is well known that the quantified determination of glucose with an enzyme-based biosensor is mainly based on the electrochemical detection of the enzymatically liberated H$_2$O$_2$. Therefore, the sensitivity of the enzyme-based biosensor is dependent on its electrochemical response to H$_2$O$_2$. That is to say, electrodes with high catalytic efficiency to H$_2$O$_2$ could also enhance the sensitivity of the biosensor to glucose [34, 10]. To investigate the biosensing ability to glucose, the enzyme electrode was prepared using the optimized cross-linking technique according to our previous work [35]. Prior to immobilization of glucose oxidase (GOx), the TiO$_2$NTs/r-GO/AgNPs nanocomposite electrode was immersed in phosphate buffer solution to generate a hydrophilic surface. The bovine serum albumin (BSA) and glutaraldehyde mixture was prepared by dissolving 25 mg BSA and 100 μL glutaraldehyde in 1 mL phosphate buffer solution. The GOx solution was prepared by dissolving 2.5 mg GOx in 100 μL phosphate buffer solution. 20 μL mixture solution of BSA and glutaraldehyde was dropped onto the prepared surface of the nanocomposite electrode. The electrode was then left in air for 10 min to dry, which also allowed BSA to adsorb onto the nanocomposite electrode. Then, 20 μL GOx solution was dropped onto the surface of the electrode. Before
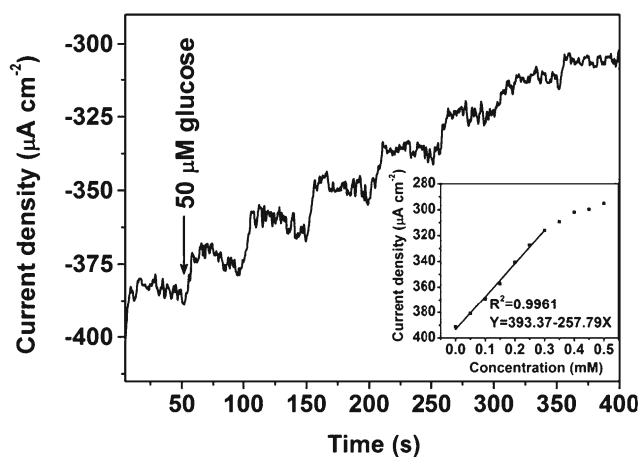
Fig. 6 Current-time responses of the enzyme electrode to successive addition of glucose in N_2-saturated 0.2 M phosphate buffer solution (pH 6.8) under an applied potential of -0.6 V (vs. SCE); Inserted graph shows the calibration curve of the enzyme electrode as a function of glucose concentration

electrochemical experiments, the enzyme electrode was washed with phosphate buffer solution to remove the unimmobilized GOx and stored in dry condition at 4 °C before use.

Amperometric detection of glucose using the enzyme electrode

The cyclic voltammetric measurements of enzyme electrode were carried out in N_2-saturated phosphate buffer solution containing different concentration of glucose (0–1,000 μM glucose) (Fig. S9, ESM). It can be seen that the reductive current at about -0.6 V decreased with the increase of glucose concentration. The typical amperometric responses at the enzyme electrode for each successive addition of 50 μM glucose were shown in Fig. 6. The corresponding calibration curve was shown in the insert of Fig. 6. It can be seen that the biosensor showed a sensitive response to glucose in the concentration range 50~0.5 mM. The amperometric response to glucose at -0.6 V exhibited a linear relationship in glucose concentration of 50~300 μM (correlation coefficient R^2, 0.9961). The corresponding sensitivity of the glucose biosensor was 257.79 μA mM^{-1} cm^{-2}. Table S3 in ESM displayed the sensitivity of the enzyme electrode with other glucose sensors based on recently reported nanocomposite materials. It was evident that the sensitivity of our enzyme electrode was significantly higher than that of other glucose sensors. It means that the prepared enzyme biosensor also had a potential application in the determination of glucose. Therefore, such TiO$_2$NTs/r-GO/AgNPs nanocomposites may possess great prospect for applications in areas of analytical chemistry and clinical medicine.

Conclusions

The TiO$_2$NTs/r-GO/AgNPs nanocomposite was fabricated for electrochemical sensing of hydrogen peroxide. The r-GO modification on surface of the TiO$_2$NTs was used to prevent the aggregation of chemi-deposited AgNPs. The nanocomposite electrode exhibited a high electrochemical catalytic activity for H$_2$O$_2$ detection. A high sensitivity of 1151.98 μA mM^{-1} cm^{-2} and a wide linear range of 50~15.5 mM were obtained. Additionally, the nanocomposite electrode was also used for fabrication of glucose biosensor via immobilizing GOx onto its surface. The glucose biosensor exhibited a good sensing performance for glucose detection. Furthermore, the experimental results demonstrated that the r-GO modification on surface of the TiO$_2$NTs was an effective method for preventing the AgNPs aggregation. Accordingly, the approach in the present work could provide a way to construct more TiO$_2$NTs/r-GO-based nanocomposites for other electrochemical applications.

References

1. Jang HD, Kim SK, Chang H, Roh K-M, Choi J-W, Huang J (2012) A glucose biosensor based on TiO$_2$-graphene composite. Biosens Bioelectron 38(1):184–188
2. Li J, Kuang D, Feng Y, Zhang F, Liu M (2012) Glucose biosensor based on glucose oxidase immobilized on a nanofilm composed of mesoporous hydroxyapatite, titanium dioxide, and modified with multi-walled carbon nanotubes. Microchim Acta 176(1–2):73–80
3. Xie Y, Zhou L, Huang H (2007) Bioelectrocatalytic application of titania nanotube array for molecule detection. Biosens Bioelectron 22(12):2812–2818
4. Lu X, Wang G, Zhai T, Yu M, Gan J, Tong Y, Li Y (2012) Hydrogenated TiO2 nanotube arrays for supercapacitors. Nano Lett 12(3):1690–1696
5. Xie Y, Zhao Y (2013) Electrochemical biosensing based on polypyrrole/titania nanotube hybrid. Mater Sci Eng C 33(8):5028–5035
6. Du H, Xie Y, Xia C, Wang W, Tian F (2014) Electrochemical capacitance of polypyrrole-titanium nitride and polypyrrole-titania nanotube hybrids. New J Chem 38(3):1284–1293
7. Xie Y, Wang Y, Du H (2013) Electrochemical capacitance performance of titanium nitride nanoarray. Mater Sci Eng B 178(20):1443–1451
8. Xia C, Xie Y, Wang Y, Wang W, Du H, Tian F (2013) Preparation and capacitance performance of polyaniline/titanium nitride nanotube hybrid. J Appl Electrochem 43(12):1225–1233

9. Xie Y, Fang X (2014) Electrochemical flexible supercapacitor based on manganese dioxide-titanium nitride nanotube hybrid. Electrochim Acta 120:273–283

10. Jiang Y, Zheng B, Du J, Liu G, Guo Y, Xiao D (2013) Electrophoresis deposition of Ag nanoparticles on TiO2 nanotube arrays electrode for hydrogen peroxide sensing. Talanta 112:129–135

11. Kafi AKM, Wu G, Chen A (2008) A novel hydrogen peroxide biosensor based on the immobilization of horseradish peroxidase onto Au-modified titanium dioxide nanotube arrays. Biosens Bioelectron 24(4):566–571

12. Kong L, Lu X, Bian X, Zhang W, Wang C (2010) A one-pot synthetic approach to prepare palladium nanoparticles embedded hierarchically porous TiO2 hollow spheres for hydrogen peroxide sensing. J Solid State Chem 183(10):2421–2425

13. Arif Sher Shah MS, Zhang K, Park AR, Kim KS, Park N-G, Park JH, Yoo PJ (2013) Single-step solvothermal synthesis of mesoporous Ag-TiO2-reduced graphene oxide ternary composites with enhanced photocatalytic activity. Nanoscale 5(11):5093–5101

14. German N, Ramanaviciene A, Voronovic J, Ramanavicius A (2010) Glucose biosensor based on graphite electrodes modified with glucose oxidase and colloidal gold nanoparticles. Microchim Acta 168(3–4):221–229

15. Zhang Z, Xu F, Yang W, Guo M, Wang X, Zhang B, Tang J (2011) A facile one-pot method to high-quality Ag-graphene composite nanosheets for efficient surface-enhanced Raman scattering. Chem Commun 47(22):6440–6442

16. Fan J, Shi Z, Ge Y, Wang J, Wang Y, Yin J (2012) Gum arabic assisted exfoliation and fabrication of Ag–graphene-based hybrids. J Mater Chem 22(27):13764–13772

17. Badawy AME, Luxton TP, Silva RG, Scheckel KG, Suidan MT, Tolaymat TM (2010) Impact of environmental conditions (pH, ionic strength, and electrolyte type) on the surface charge and aggregation of silver nanoparticles suspensions. Environ Sci Technol 44(4):1260–1266

18. Pérez-López B, Merkoçi A (2012) Carbon nanotubes and graphene in analytical sciences. Microchim Acta 179(1–2):1–16

19. Wang Q, Yun Y (2013) Nonenzymatic sensor for hydrogen peroxide based on the electrodeposition of silver nanoparticles on poly(ionic liquid)-stabilized graphene sheets. Microchim Acta 180(3–4):261–268

20. Moradi Golsheikh A, Huang NM, Lim HN, Zakaria R, Yin C-Y (2013) One-step electrodeposition synthesis of silver-nanoparticle-decorated graphene on indium-tin-oxide for enzymeless hydrogen peroxide detection. Carbon 62:405–412

21. Gong H, Sun M, Fan R, Qian L (2013) One-step preparation of a composite consisting of graphene oxide, Prussian blue and chitosan for electrochemical sensing of hydrogen peroxide. Microchim Acta 180(3–4):295–301

22. Chang Q, Tang H (2014) Optical determination of glucose and hydrogen peroxide using a nanocomposite prepared from glucose oxidase and magnetite nanoparticles immobilized on graphene oxide. Microchim Acta:1–8

23. Liu C, Teng Y, Liu R, Luo S, Tang Y, Chen L, Cai Q (2011) Fabrication of graphene films on TiO2 nanotube arrays for photocatalytic application. Carbon 49(15):5312–5320

24. Yun J-H, Wong RJ, Ng YH, Du A, Amal R (2012) Combined electrophoretic deposition–anodization method to fabricate reduced graphene oxide–TiO2 nanotube films. RSC Adv 2(21):8164–8171

25. Song P, Zhang X, Sun M, Cui X, Lin Y (2012) Graphene oxide modified TiO2 nanotube arrays: enhanced visible light photoelectrochemical properties. Nanoscale 4(5):1800–1804

26. Zhao H, Fu H, Zhao T, Wang L, Tan T (2012) Fabrication of small-sized silver NPs/graphene sheets for high-quality surface-enhanced raman scattering. J Colloid Interface Sci 375(1):30–34

27. Ahmad M, Ahmed E, Hong ZL, Khalid NR, Ahmed W, Elhissi A (2013) Graphene-Ag/ZnO nanocomposites as high performance photocatalysts under visible light irradiation. J Alloys Compd 577:717–727

28. Jin Z, Nackashi D, Lu W, Kittrell C, Tour JM (2010) Decoration, migration, and aggregation of palladium nanoparticles on graphene sheets. Chem Mater 22(20):5695–5699

29. Cai W, Piner RD, Stadermann FJ, Park S, Shaibat MA, Ishii Y, Yang D, Velamakanni A, An SJ, Stoller M, An J, Chen D, Ruoff RS (2008) Synthesis and solid-state NMR structural characterization of 13C-labeled graphite oxide. Science 321(5897):1815–1817

30. Tan E-Z, Yin P-G, T-t Y, Wang H, Guo L (2012) Three dimensional design of large-scale TiO2 nanorods scaffold decorated by silver nanoparticles as SERS sensor for ultrasensitive malachite green detection. ACS Appl Mater Interfaces 4(7):3432–3437

31. Tung VC, Allen MJ, Yang Y, Kaner RB (2009) High-throughput solution processing of large-scale graphene. Nat Nanotechnol 4(1):25–29

32. Alwarappan S, Liu C, Kumar A, Li C-Z (2010) Enzyme-doped graphene nanosheets for enhanced glucose biosensing. J Phys Chem C 114(30):12920–12924

33. Gu Z, Yang S, Li Z, Sun X, Wang G, Fang Y, Liu J (2011) An ultrasensitive hydrogen peroxide biosensor based on electrocatalytic synergy of graphene-gold nanocomposite, CdTe-CdS core-shell quantum dots and gold nanoparticles. Anal Chim Acta 701(1):75–80

34. Garjonyte R, Malinauskas A (2000) Amperometric glucose biosensors based on Prussian blue- and polyaniline-glucose oxidase modified electrodes. Biosens Bioelectron 15(9–10):445–451

35. Wang W, Xie Y, Wang Y, Du H, Xia C, Tian F (2014) Glucose biosensor based on glucose oxidase immobilized on unhybridized titanium dioxide nanotube arrays. Microchim Acta 181(3–4):381–387